Research Article

Balaji Rao Pradeepa and Amirthalingam V. Kiruthika*

Preparation and characterization of sisal fibre reinforced sodium alginate gum composites for non-structural engineering applications

https://doi.org/10.1515/epoly-2023-0027
received April 03, 2023; accepted June 10, 2023

Abstract: In this work, untreated/treated sisal fibre (SF)-reinforced sodium alginate composites for three different concentrations (1.5%, 2%, and 2.5%) are fabricated by the hand lay-up method, and the variations in mechanical properties such as tensile strength, flexural strength, and impact strength are studied. The treated and untreated composites are analysed and compared using scanning electron microscope to study the surface morphology. Energy-dispersive spectroscopic analysis is carried out to evaluate the elemental compositions. Fourier transform infrared spectroscopic analysis is conducted to determine the interaction between fibres and matrix material. The thermal observations such as differential scanning calorimetry and thermogravimetric analysis showed only slight variations between the untreated and treated SF composites. The results of this work indicate that untreated sample with the maximum sodium alginate gum concentration had significantly enhanced mechanical properties and low moisture absorption rate. Biodegradation test inferred that it was superior for the treated fibre rather than the untreated fibre composites. The primary objective of this work is to assess the suitability of these composites for non-structural engineering applications.

Keywords: sisal fibre, sodium alginate, tensile strength, soil burial, scanning electron microscopy

1 Introduction

In recent years, biodegradable composites have garnered a significant attention, primarily for applications in a variety of industrial sectors. Furthermore, the depletion of petroleum resources and worldwide environmental concerns need the development of new green materials that are biodegradable and eco-friendlier (1). Biodegradable composites have the greater potential in the utilization of plant fibres as reinforcing material due to their recyclability, inexpensive, biodegradability, naturally occurring abundance, specific mechanical characteristics, etc. Compared to synthetic (traditional) fibres such as carbon, Kevlar, glass, and aramid, the plant fibres are sustainable, non-toxic, and have been proven to be more effective in the field of lightweight engineering (2). In general, it is quite difficult to dispose of synthetic polymer composites, and the use of plastic has been outlawed. As a result, there is a greater need today for the plant fibres as an alternative to the synthetic fibres in a variety of disciplines (3).

Plant fibres are lignocellulose in nature, which absorb moisture and are used in packaging, vibration isolators, and roofing sheets. The main disadvantages of these fibres are less adherence with the matrix due to their matrix's hydrophobicity and hydrophilic nature of fibres. Thus, weak fibre matrix lowers the fibre's reinforcing behaviour, thus preventing stress transfer from the matrix to load-carrying fibres. In order to find a solution to the aforesaid issues, researchers used various chemical treatments (silane, alkali, permanganate, isocyanate), incorporation of filler substances into matrix, and hybridization (with other plant fibres or filler or conventional fibres) (4).

Numerous researchers used different kinds of plant fibres such as jute (5), bamboo (6,7), hemp (8), flax (9), and kenaf (10), obtained from the plant's stem, sisal (11–13), pine apple leaf fibre (14), abaca (15), from the leaf and coir (16,17), cotton (18) from the fruit of the plant. Sisal, a hard fibre that belongs to *Agave sisalana*, received greater attention, because of their lightweight, easy availability, and low

*** Corresponding author: Amirthalingam V. Kiruthika,** Department of Physics, Seethalakshmi Achi College for Women (Affiliated to Alagappa University, Karaikudi), Pallathur, Tamil Nadu, 630107, India, e-mail: avkiruthi@gmail.com
Balaji Rao Pradeepa: Department of Physics, Seethalakshmi Achi College for Women (Affiliated to Alagappa University, Karaikudi), Pallathur, Tamil Nadu, 630107, India

thermal conductivity. A good sisal plant is about 1 m tall, 28 mm wide, and yields 200–250 leaves (19). Each leaf has 1,000–1,200 fibre bundles, which contain 4% of fibres, moisture content of 87.25%, cuticle of 0.75%, and other matters of 8%. Sisal fibre (SF) consists of porosity (17%), density (1.45 g·cm^{-3}), spiral angle (20–25°), diameter (21.5 × 10^{-3}), and crystallinity (62.8%). The physico-mechanical properties of SF have been highly dependent on source, age, location, fibre diameter, gauge length, extracting techniques, and strain ratio. SFs are potential reinforcements in various resins, elastomers, and other types of polymeric systems (20).

On the other hand, sodium alginate (NaAg), a biodegradable polymer used for this study, could replace commodity petro-based plastics. NaAg, a linear natural polysaccharide, is obtained from marine brown algae, and it consists of 1,4-β-D-mannuronic acid (M) and α-L-guluronic acid (G). Alginate can be determined by its M/G ratio and its molecular weight. The M/G units create random arrangements of MM, GG, and MG blocks. By increasing the length of their G block and molecular weight, the mechanical properties of NaAg gels have been increased (21). The gel is an ionic polyelectrolyte and has widespread applications in wastewater treatment (22), wound dressing, tissue engineering, antimicrobial and antiviral activities, cosmeto textiles, sensors, etc. (23–25).

For the past two decades, extensive research works have been carried out to investigate the various characteristics of SF-reinforced polymer composites. The effect of various concentrations of matrix, fibre loading, and fibre length influenced the physico-mechanical behaviours of composites. Samouh et al. (26) reported that the increase in the rate of reinforcement (fibre) enhanced the mechanical and dynamic mechanical properties of SF/polylactic acid (PLA) composites. Since the SF served as a nucleating agent for PLA, increasing their concentration in the matrix increased the degree of crystallinity from 47% to 61%. Chemical treatment played an important role in determining the mechanical strength of the composites. Adane and Awoke (27) characterized the chemically treated SF/polyester composites, and the results revealed that the treated SF composites have better mechanical properties and low water absorption than the untreated fibre composites. The similar results were observed by Agernew et al. (28), who found that alkali treatment enhanced the mechanical strength with an increase in fibre content. Parul and Gupta (29) studied the influence of alkali treatment and PLA coating as a new treatment on mechanical properties of sisal composites, and the results inferred that treated SF composites showed higher value of storage modulus and mechanical strength than the untreated one.

The purpose of this investigation is to prepare the effect of alkali treatment on the SF-reinforced NaAg composites. The mechanical, thermal, and morphological properties of alkali-treated composites with the effect of various matrix concentrations are studied. In addition, the result of the mechanical strength of treated composites is compared to that of the untreated one. At the end of soil burial, Fourier transform infrared (FTIR), differential scanning calorimetry (DSC), thermogravimetric analysis (TGA), scanning electron microscope (SEM), and moisture absorption (MA) tests are carried out.

2 Materials and methods

SFs were purchased from Wholesale Trader, Tamil Nadu, India. The length of the SFs obtained was 1 m. NaAg powder and sodium hydroxide (NaOH) in pellet form were supplied by Shri Balaji Scientific Company, Tamil Nadu, India. The properties of NaAg and SF are presented in Table 1.

2.1 Fibre surface treatment

Raw SFs were treated with 5% NaOH (alkali solution) and were continuously heated to 80°C for 3 h, thereby maintaining the material-to-liquid ratio of 1:30. The fibres were thoroughly rinsed with water to eliminate any residues of alkali that may have been present on the fibre surface and achieve a pH level of 7. The treated fibres were then dried at room temperature (32°C) for 24 h (30). The untreated and alkali-treated fibres chopped in the range of 10 mm were used for this study.

2.2 Preparation of NaAg gum

In order to make the matrix material for the composite structure, NaAg powder and distilled water were used as

Table 1: Material properties of NaAg and SF

Materials		Parameters
NaAg	Viscosity of 2% aqueous solution at 20°C	1,000–1,200 cPs
	Bulk density	0.9090 g·mL^{-1}
	Tapped density	0.9523 g·mL^{-1}
SF	Density (untreated)	1.46 g·cm^{-3}
	Density (treated)	1.66 g·cm^{-3}
	Moisture absorption	6.9088%

the two primary components. Subsequently, the NaAg gum solution was prepared at three discrete concentrations, namely 1.5%, 2%, and 2.5%. To prepare the matrix material, it was recommended that NaAg powder was mixed with distilled water at room temperature (32°C) and stirred continuously for 45 min to prevent the formation of agglomerates or stratification on the surface. Then, the solution was subjected to centrifugation for 10 min at a speed of 3,000 rpm to remove any undissolved particles present in the gum solution.

2.3 Fabrication of composites

The composite specimens were prepared for untreated and treated SFs with NaAg solution of various concentrations (1.5%, 2%, and 2.5%) using the hand lay-up process. About 10 g of fibre was taken and cut into small pieces of the order of 10 mm in length. The material-to-composite preparation ratio was 1:20 (SF:NaAg). The fibres were spread on the plastic tray, and 200 mL of NaAg solution having 1.5% concentration was poured over the fibre and intermixed manually. The fibre–gum mixture was dried under sunlight for 10–20 h depending on the atmospheric condition. A typical view of steps involved in the preparation of composites is shown in Figure 1. The prepared material does not yield considerable strength. In order to increase the mechanical characteristics, humidification cum compression techniques were used. Similar procedure was adopted for the preparation of SFC with the other concentrations of NaAg (2% and 2.5%). U1, U2, and U3 samples represented the untreated SF composites and T1, T2, T3 were the treated SF composites with NaAg concentrations at 1.5%, 2%, and 2.5%. Similarly, UH1, UH2, and UH3 were the untreated SFs and TH1, TH2, and TH3 were the treated SFs with heating the solution of NaAg at 1.5%, 2%, and 2.5% concentrations, respectively.

2.4 Mechanical properties

The tensile and flexural properties of the composites were investigated by Tinius Olsen H10KL at a crosshead speed of 2 mm·min^{-1}. Five samples were tested, and the average values were reported for the untreated and treated SFC. From the stress–strain curve, the tensile strength (maximum force/cross-sectional area of the composites) was calculated.

$$\text{Flexural strength} = \frac{3PL}{2bd^2} \tag{1}$$

where P, L, d, and b are the flexural load, length of the span, depth, and width of the composites, respectively. Impact test for the prepared composites was analysed by Tinius Olsen Model IT 504 Plastic impact testing machine. Six samples were taken, and the average was calculated for each concentration.

2.5 Soil burial test

The soil burial test of untreated/treated SF-reinforced NaAg composites was carried out in an open environment for biodegradation studies. The test samples chosen were from the SF/NaAg composite of 2.5% concentration. The natural soil biodegradation test lasted for 1 month. The ambient temperature and time during the tests were noted down. The test samples of untreated/treated SF NaAg composites were cut into a rectangular shape of size 5 cm × 3 cm pieces (approximately 2–2.5 g). The ground was dug to a depth of 35 cm. Regular weeding of the ground was done in order to maintain its quality. Each sample was buried at a depth of 35 cm below the surface of the soil. Incubation of the samples was done at a temperature of 34°C for a period of 5, 10, 15, 20, 25, and 30 days. After every 5 days, the samples were carefully removed, gently brushed to remove adhering soil, without deforming its shape, and then dried at room temperature until a constant weight was obtained. Each sample was weighed before and after degradation using a SHIMADZU digital weighing scale (0.001 g precision). Weight loss was calculated using the following relationship. Three replicates of each sample were taken for the test.

$$\text{Percentage weight loss} = \frac{W_0 - W_\text{d}}{W_0} \times 100\% \tag{2}$$

where W_0 is the initial weight of samples (g) and W_d is the weight of dried samples (g).

2.6 FTIR

The presence of interfacial bonds in the SF and composites was studied using FTIR. Using the kBr pellet, FTIR analysis was performed, and the spectrum was obtained with a resolution of 4 cm^{-1}, with the range of 400–4,000 cm^{-1}.

2.7 Morphological study

The SEM images of the untreated and treated composites were taken using JSMIT200 SEM with an accelerating

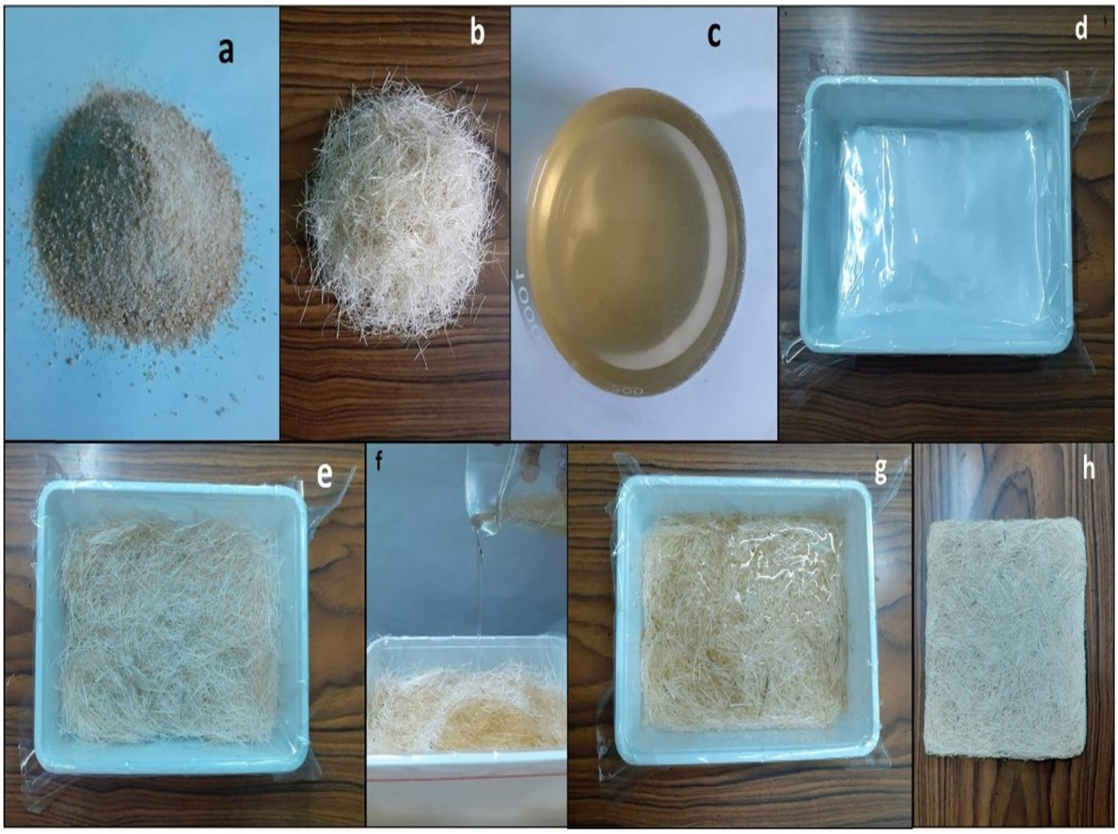

Figure 1: Procedure for the preparation of composites: (a) NaAg powder, (b) untreated SF, (c) NaAg gum solution, (d) plastic mould, (e) untreated SF in plastic mould, (f) NaAg gum solution added to untreated SF, (g) untreated SF with NaAg gum solution (wet), and (h) untreated SF/NaAg composite (dry).

voltage of 20 kV to analyse the morphological characteristics of the prepared composite. The surface of the specimen is gold-sputtered and scanned at a magnification of 1,000×.

2.8 Thermal properties

SF-treated and untreated composites with 2.5% concentration of NaAg were subjected to TGA and DSC thermograms using Perkin Elmer Simultaneous Thermal Analyser (STA6000). Samples of 5–20 mg were taken and heated at the rate of 10°C·min^{-1}. From this study, the weight loss of the composites with temperature was noted.

2.9 MA

MA of untreated and treated SF/NaAg composites has been carried out (31). Five specimens were dried and weighed in the digital balance to the nearest of 0.001 g. All the samples were kept in a humidification chamber for about 5 h at room temperature. The weight of the composites was measured after taking from the chamber. The percentage of increase in weight during the absorption of moisture was calculated.

3 Results and discussion

3.1 Mechanical properties

In order to examine the contribution of SF and the matrix concentration to the composites, the tensile characteristics were analysed. Figure 2 shows the tensile results of U1, U2, and U3 samples. The stress–strain curve was recorded for U1 to U3 samples, especially for various concentrations of NaAg (1.5%, 2%, and 2.5%). From Figure 2, it was observed that the U3 sample had the maximum strength because it has more adhesiveness with the fibre particles. This enhances the load-bearing capacity, which in turn

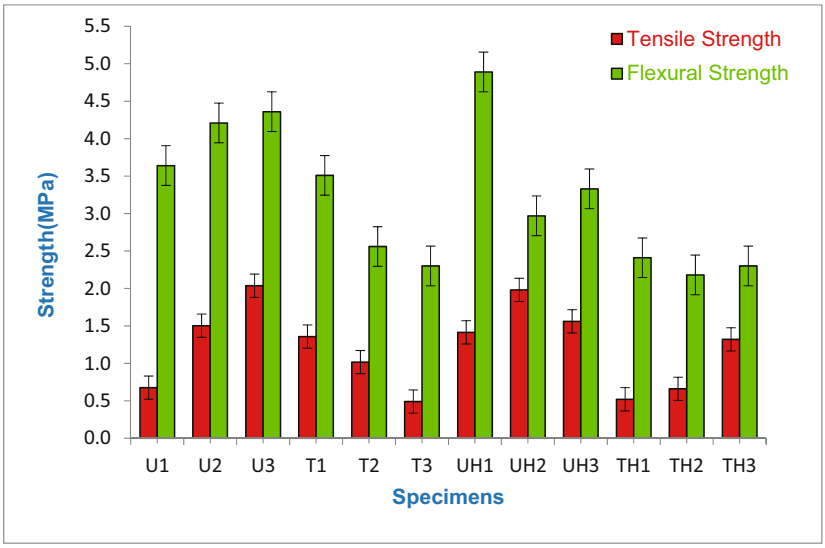

Figure 2: Tensile and flexural strength of the samples.

increases the mechanical strength of the U3 sample. In contrast, the tensile strength of the U1 and U2 samples was lower in comparison with that of the U3 samples; this is due to the fact that there was less bonding between the fibres and the matrix in the U1 and U2 samples. The U3 samples had a higher tensile strength than the U1 and U2 samples. The increase in tensile values for untreated fibre composites that occurred as a result of increasing the matrix concentration from 1.5% to 2.5% followed the order of U3 > U2 > U1.

A considerable reduction takes place in the tensile strength for the alkali-treated sisal fibre composites (SFCs). In the case of treated fibre combination, the maximum strength was achieved for T1, and the strength was reduced by 33.3%, 50.0%, and 60.0%, respectively, for T1, T2, and T3. When the concentration of the matrix was increased from 1.5% to 2.5%, the tensile values of the treated fibre composites fell, and the order of the decreases was T1 > T2 > T3. According to the findings of this study, untreated fibre composites considerably improved the strength of the material, but treated combinations had the opposite effect.

We have studied the mechanical properties of untreated and treated fibre composites that were reinforced with a heating solution of NaAg, and the results are illustrated in Figure 2. The tensile strength was gradually increased (all the way up to 2% of NaAg), and subsequently, it was lowered for UH3 sample (sample containing 2.5% concentration). UH2 and TH1 samples possesses superior strength when compared to the other combinations.

Using load vs displacement curve, the flexural property was measured with a crosshead speed of 2 mm·min^{-1}. Figure 2 displays the results of flexural testing conducted on both untreated and treated fibre composites. It was found that the prepared composites had findings for their flexural strength that are extremely similar to the results of tensile strength. According to Figure 2, the flexural strength of the U3 sample was the highest compared to that of the other combinations (U1, U2, T1, T2, and T3). On the other hand, the random intermediate flexible strength was displayed by the composites UH2, UH3, TH2, and TH3. As a result, a higher strength was noted for UH1, which pointed out to a successful coupling of untreated SF with the composite. As reported by Tengsuthiwat et al. (32), the tensile strength of poly(3-hydroxybutyrate-co-3-hydroxyvalerate)/SF composites at 5 wt% fibre loading showed 23.6 MPa, and the same results were obtained by Thorsak et al. (33). In the case of SF/PLA composite reinforced with different fibre contents (5%, 10%, and 15%), the 15% fibre loading had the greatest tensile strength of 70.76 MPa. In addition to that, the tensile strength and flexural strength were increased from 4.5 to 8.5 MPa and from 7.6 to 11.8 MPa, respectively, for SF/cassava starch-based biocomposites, and the authors concluded that the prepared materials have the possible use of low-cost housing, civil structure, and food packaging applications.

The impact test was conducted, and the results are shown in Figure 3. Impact resistance is the material's capacity to withstand breaking when subjected to sudden mechanical load, such as when a pendulum hits the surface of a composite (34). It is clear from Figure 3 that impact strength was increased with increasing NaAg concentration. Like tensile and flexural strength, the impact was also found maximum for the U3 sample. Because of the strong interfacial adhesion that existed between the SF

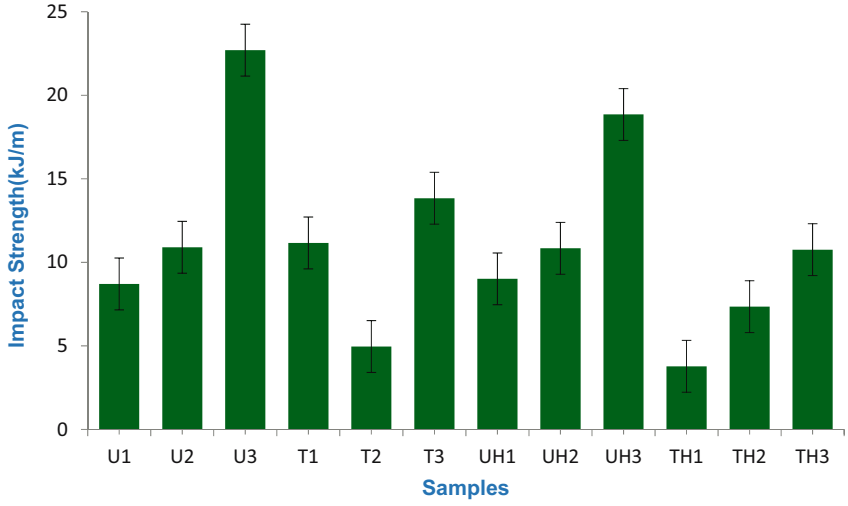

Figure 3: Impact strength of the samples.

and the NaAg concentration (at 2.5%), the U3 specimen was able to absorb a greater portion of the impact load. Therefore, the 2.5% concentration of NaAg reinforced with untreated and treated SF demonstrated higher impact strength compared to the 1.5% and 2% concentrations of NaAg for all specifications. This was the case for both the solution of NaAg that was heated and the solution of NaAg when it was not heated. The untreated SFC that was reinforced with a 2.5% concentration of NaAg solution exhibited favourable results for its mechanical properties, including tensile, flexural, and impact strengths. Based on the findings of this research, it is determined that the treatment with alkali reduces the strength of the composites. This was attributed to the fact that the alkali treatment diminished the hydrophilic characteristics of SF, and as a result, hydrophilic NaAg served as the good reinforcement to the composites. Ismail et al. (35), who conducted the research work on mechanical properties of kenaf fibre/epoxy composites, noted the similar pattern. The impact strength of the SF-reinforced cassava starch biocomposites was studied by Siddesh et al. (36). The results showed that increasing fibre length from 5 to 20 mm increased the impact strength from 4.1 to 5.2 $kJ{\cdot}m^{-2}$, respectively, and suddenly decreased the strength (4.8 $kJ{\cdot}m^{-2}$) for 25 mm fibre length. Samouh et al. (26) studied the impact strength of SF/PLA composites is 3.87 $kJ{\cdot}m^{-2}$ (at 15% fibre loading) and concluded in their studies that increasing the fibre content (from 5% to 15%) increased the impact strength of the composites.

Composites prepared with plant fibre (sisal, flax, jute, kenaf, banana, pineapple leaf, hemp)-reinforced natural polymer (PLA, cassava starch, cellulose) exhibited a high level of tensile, flexural, and impact strengths as well as good thermal stability, when compared to the SF/NaAg composites. However, the challenges lie in the rate of biodegradation after the end-of-life that presents a number of issues. From the literature, it was observed that the biodegradation rate of PHBV/peach palm particles (37), PLA/chitosan (38–40), flax fibre/PLA (41), vetiver grass/PLA (42), and polyhydroxyalkanoates (43) composites took the duration of over 5 months, 150 days, 50 days, 180 days, and 120 days, respectively. On the other hand, the composites that we developed have a lower strength than the aforementioned material, but SF/NaAg composites are completely biodegradable and user-friendly with a soil biodegradation rate of 30 days. The main contribution of the current work is the availability of both SF and matrix in nature, and the composites that have been made are light in weight, biodegradable, and inexpensive, which makes them useful for a wide range of engineering applications.

3.2 Soil burial test

The biodegradation of a material depends on the living organisms (micro/macro), the pH value of the soil, temperature, moisture, and humidity of the environment. Also, the degradation rates are dependent on the type (treated/untreated) and nature of the material preferred. In this work, the biodegradation behaviour of the U3 and T3 composites of maximum concentration of 2.5%, after a period of 1-month soil burial test, has been investigated. The result showed that both untreated and treated SF/NaAg composites were able to degrade. However, the biodegradation rate showed a variation for the untreated/treated SF/NaAg biocomposites. It was observed that the treated SF/NaAg biocomposites (T3) are more easily biodegraded than untreated SF/NaAg composites (U3), as they are

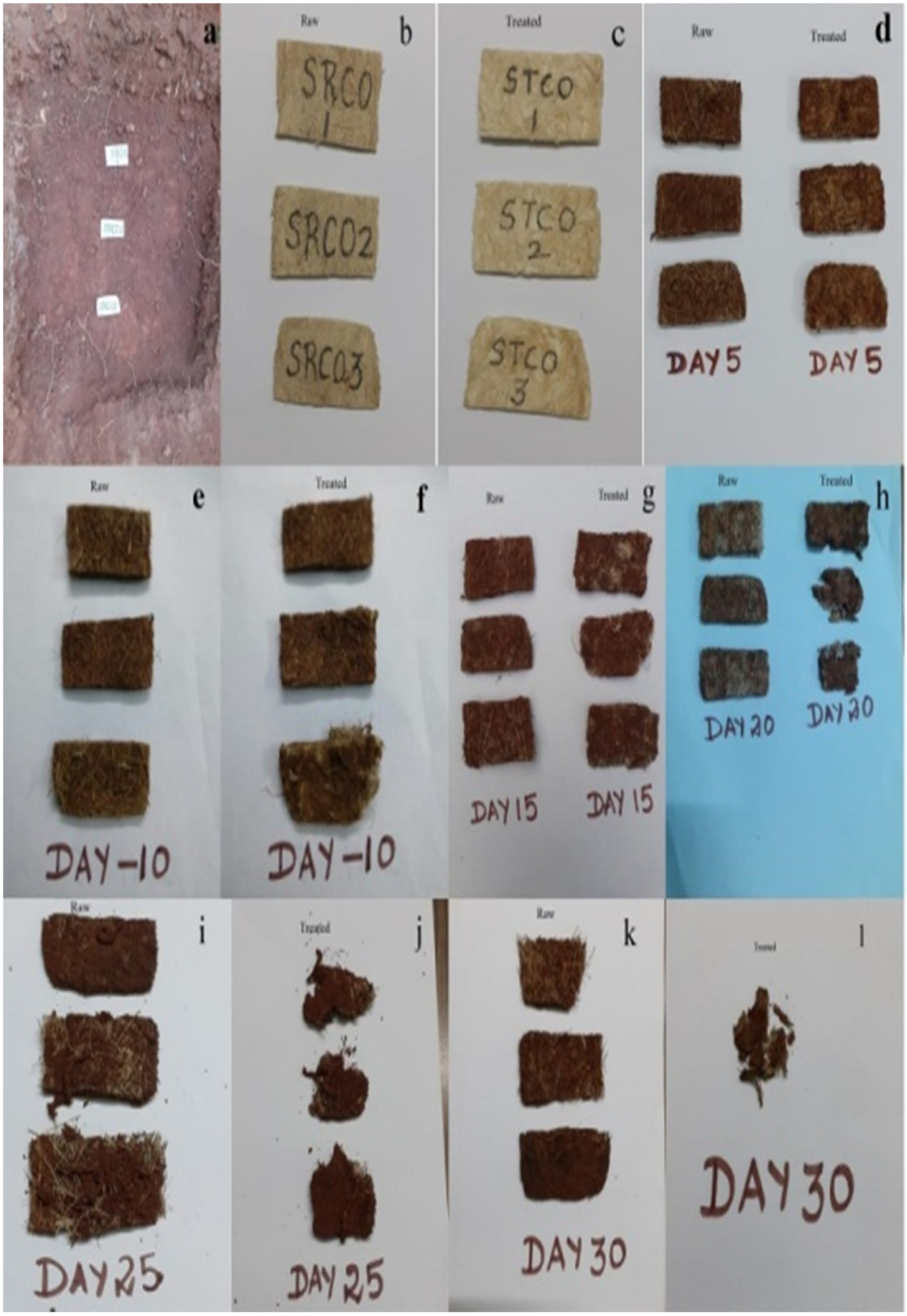

Figure 4: The U3 (raw/untreated) and T3 (treated) samples in burial pit from day 1 to 30: (a) samples placed in pit for soil burial test, (b) SRCO represents U3 sample, (c) STCO represents T3 sample, (d) U3 and T3 samples after 5 days of soil burial test, (e and f) U3 and T3 samples after 10 days, (g) samples after 15 days, (h) samples after 20 days, (i and j) samples after 25 days, and (k and l) samples after 30 days.

consumed easily by living organisms (Figure 4) that exist in the soil. The reduction in the percentage weight loss of untreated/treated SF-NaAg biocomposites in the natural

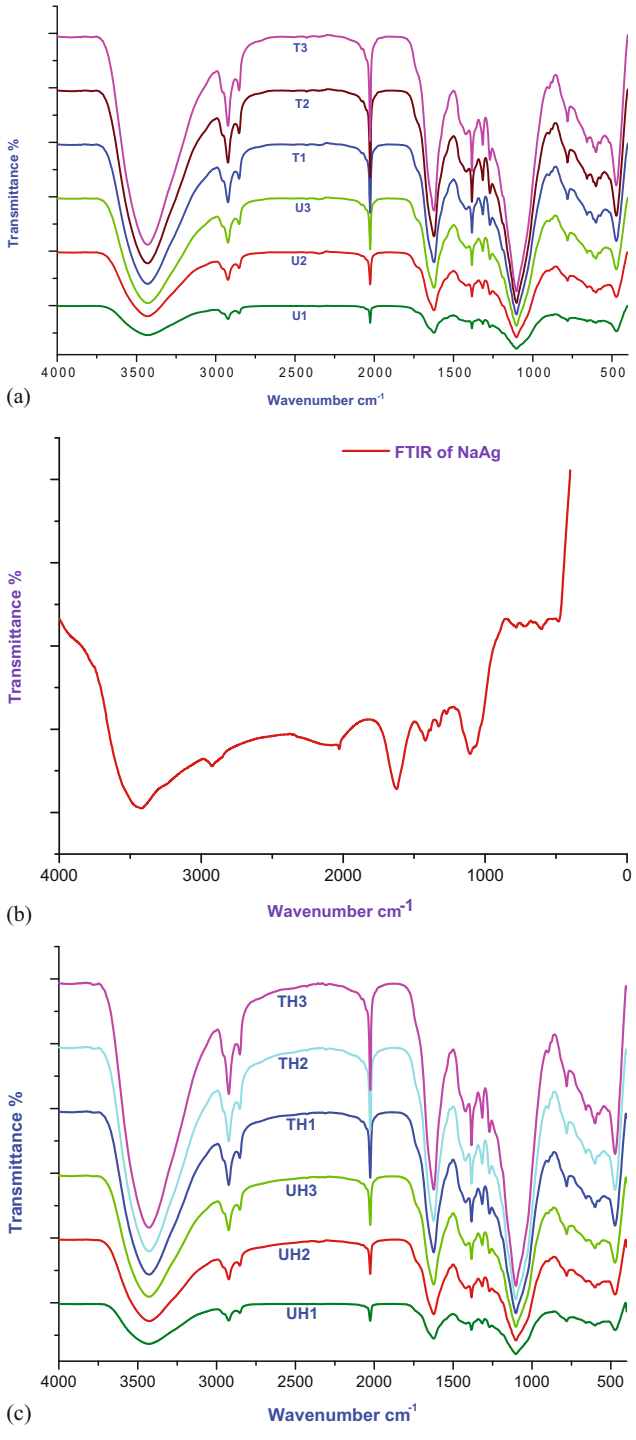

Figure 5: (a) FTIR of untreated and treated SFC without heating the NaAg solution; (b) FTIR of NaAg powder; and (c) FTIR of untreated and treated SFC with heating the NaAg solution.

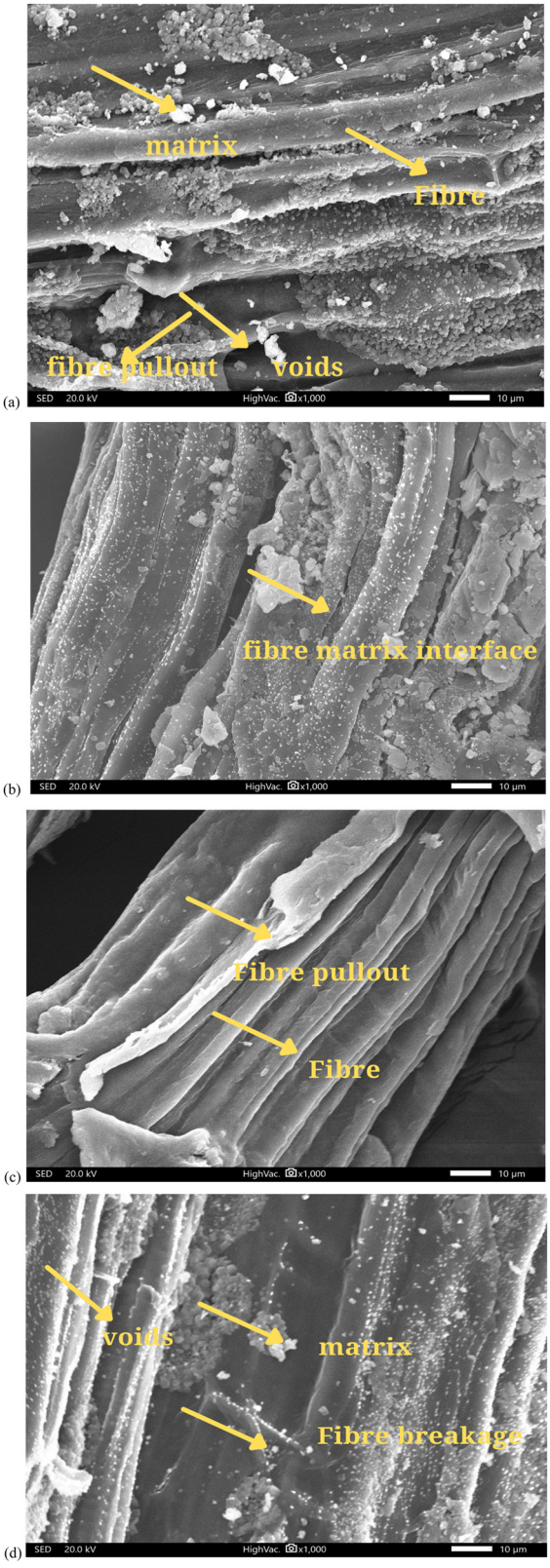

Figure 6: SEM images of (a) U3 sample, (b) T3 sample, (c) UH3 sample, and (d) TH3 sample.

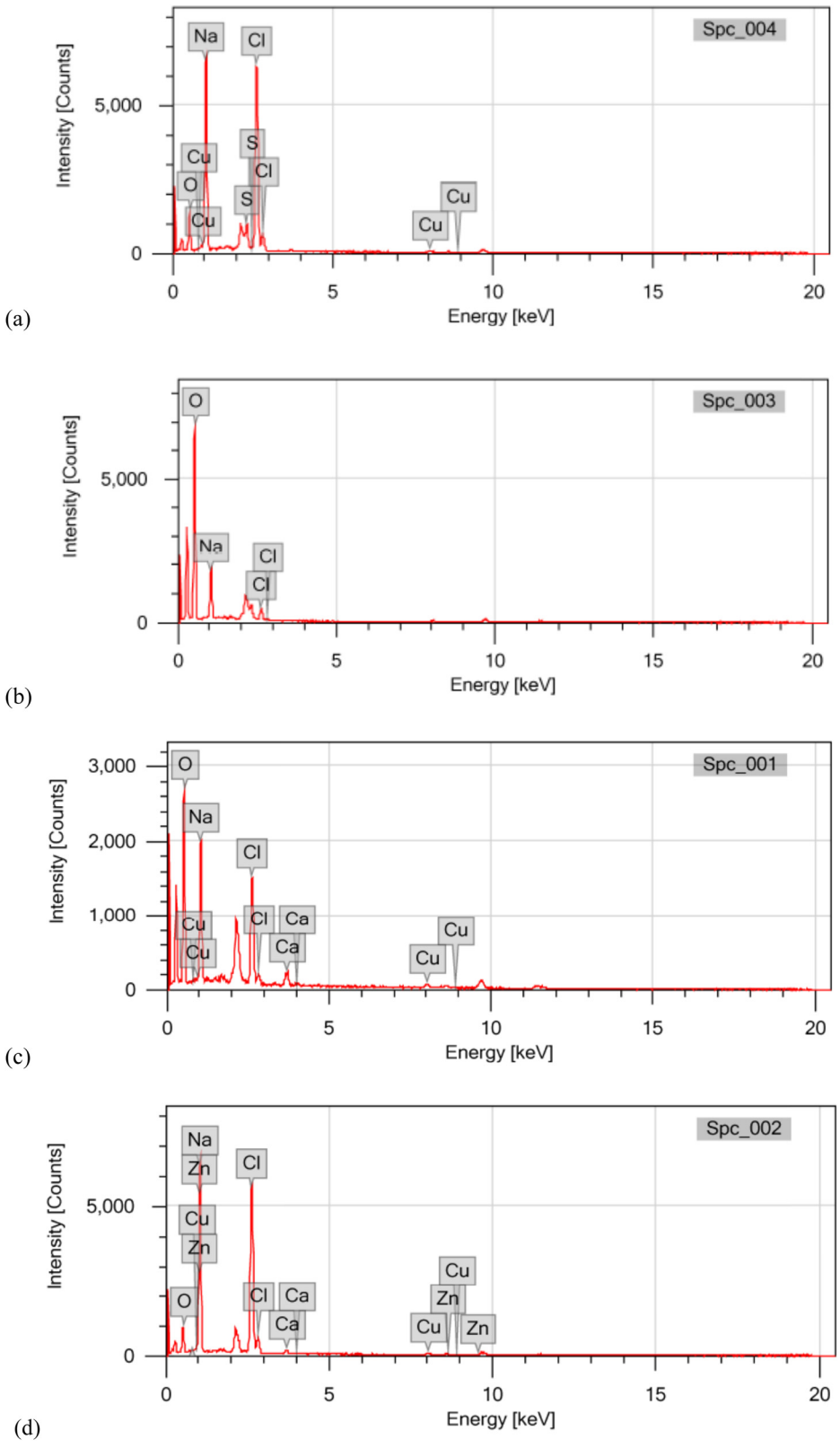

Figure 7: EDS of (a) U3 sample, (b) T3 sample, (c) UH3 sample, and (d) TH3 sample.

Table 2: Elemental compositions of the composites (%)

Sample code	O	Cl	Na
U3	18.26	40.99	35.12
T3	69.82	5.20	24.99
UH3	47.89	18.43	27.13
TH3	14.71	41.76	38.61

soil burial test was also due to temperature and humidity conditions of the environment to which the biocomposites were exposed.

3.3 FTIR

The untreated and treated SFCs were subjected to FTIR spectroscopy for the purpose of conducting research on the chemical linkages that are inherent in the composites. FTIR spectra and the corresponding transmittance peaks are illustrated in Figure 5. The spectra showed the characteristic absorption peaks in the regions of 3,400–2,860 and 2,025–400 cm^{-1}, respectively. Seven prominent vibrating bands are observed for all the composites, which are shown in Figure 5a. The characteristic peaks appeared in the region 3,428–3,433 and 2,922 cm^{-1}, which were due to the O–H and C–H stretching vibrations of cellulosic SF. The spectral bands at 1,620 cm^{-1} (vibration of water molecules absorbed in cellulose) (44) and 1,383 cm^{-1} were attributed to C–O stretching and CH bending vibrations, respectively. The peaks observed at 1,420, 1,268, to 1,105 cm^{-1} was due to the CH_2 deformation and C–O–H stretching in cellulose, respectively. Similarly, FTIR spectra were taken for NaAg in the powder form, which are shown in Figure 5b. The major peaks in the wavenumber range of 3,419, 2,922, 1,326, and 1,105 cm^{-1} were attributed to the OH, CH stretching, CH bending, and C–O–C stretching vibrations in NaAg. In general, it was observed that the FTIR spectra for untreated/treated SFCs with and without heating the NaAg solution were substantially identical (Figure 5c).

3.4 SEM

SEM images are used to analyse the internal structure, fibre pullouts, and interfacial adhesion of the composites. It was carried out on the U3 and T3 composites, at a higher concentration (2.5%) of samples. Figure 6a displays the scanning electron micrograph that was taken of the U3 sample. The presence of NaAg gum across the fibre was observed, and there was strong interfacial adhesion between the fibre and the NaAg. It is possible that this is the reason why the U3 sample has such a remarkable mechanical strength, that is, the maximal load was transmitted from NaAg to SF in the composites. In the T3 composite, there was evidence of both fibre breakage and poor adhesion (Figure 6b). Incomplete distribution of SF and NaAg can be seen in the UH3 sample (Figure 6c), whereas greater agglomeration and voids (factors that reduce strength) were also available in the TH3 material (Figure 6d).

Energy-dispersive X-ray spectroscopy is a common technique that can be used to determine the elemental compositions of a given sample even in micrometres (45). Figure 7 shows the compositions along with their distributions for both treated (T3) and untreated (U3) SFCs. It was seen that the composites contain traces of oxygen, chlorine, and sodium in their weight percentages. Table 2 presents the results of an energy-dispersive spectroscopy analysis performed on composites. This analysis reveals that the cellulosic fibre distribution in the composites contains the highest weight percentage of oxygen, chlorine, and sodium.

3.5 TGA

TGA was carried out to ascertain the thermal stability, weight loss, and thermal degradation of the prepared composites in relation to temperature. Table 3 indicates the initial and final degradation temperature as well as char residues (at 610°C), and also, the associated TGA curves are

Table 3: TGA data of the composites

Sample code	Initial temperature (°C)	Final temperature (°C)	Degradation temperature (°C)	Char residues (%)
U1	180	345	303	10.5
U2	181	340	316	35.5
U3	180	354	331	37.3
T1	182	361	324	29.6
T2	182	357	324	33.1
T3	181	354	324	24.8

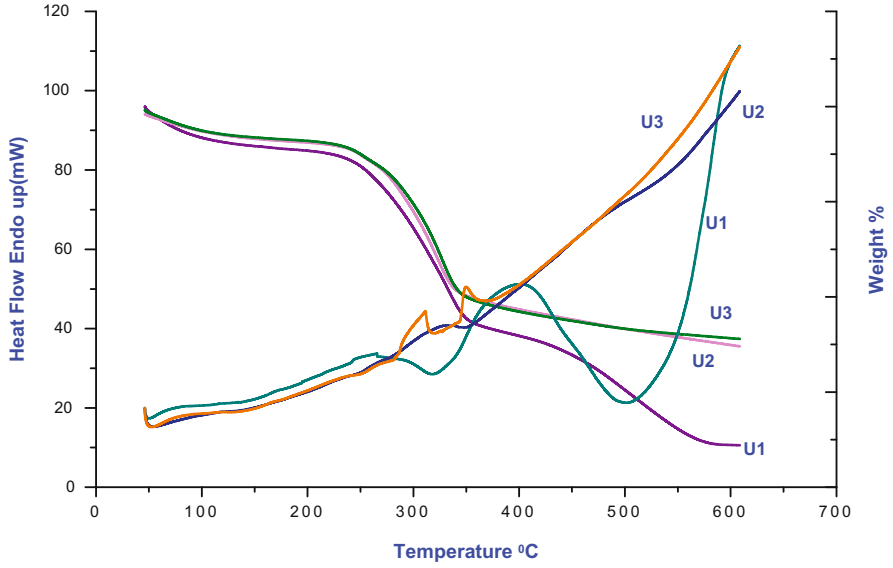

Figure 8: TGA and DSC curves of U1 to U3 samples.

detailed in Figure 8. Initial weight loss of the samples in the range of 40–140°C was accounted for the evaporation of water molecules. Simultaneously, the weight loss from 180°C to 338°C was due to the thermal degradation of chemical constituents such as cellulose, hemicellulose, and lignin that were present in the SF. At a temperature of 360°C, the final degradation takes place, which indicates the removal of the carboxyl group and the decomposition of the NaAg gum. According to the results from the TGA curve at 610°C, the char content (made of organic material) of U1, U2, and U3 samples was found to be 10.5%, 35.5%, and 37.3%, respectively. According to Kumaran et al. (46), the treated portunus shell powder-based jute fabric-reinforced epoxy composites have the maximum char residue of 35%, which indicates that portunus powder has a high molecular weight and experiences less degradation. Although each composite (U1 to U3) followed a similar pattern in terms of the temperature at which it degraded but varied in the char residues obtained. The U1 composites have a lower level of stability, and the char remains 10.5%. As a result, the composites followed the lower thermal stability in the order of U3 > U2 > U1.

The alkali treatment of SFC could influence the thermal analysis (Figure 9) of composites (T1 to T3) to

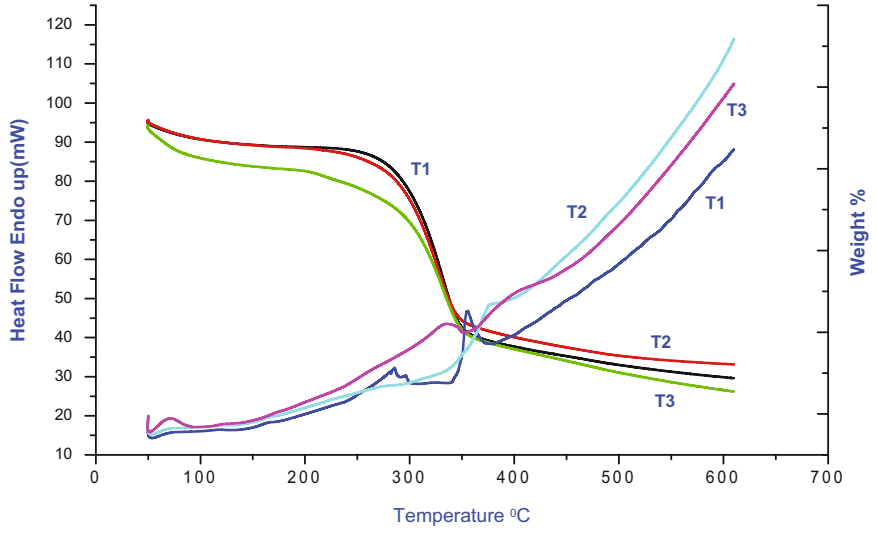

Figure 9: TGA and DSC curves of T1 to T3 samples.

some extent, and the degradation process occurs as similar to U3. The less incompatibility between the alkali-treated SF and the soluble matrix decreases the thermal stability when compared to U1, U2, and U3. The char residues of T1, T2, and T3 were 29.6%, 33.1%, and 24.8%, respectively, at 640°C.

3.6 DSC

The process of releasing or absorbing heat energy for the prepared composites was done by DSC. In addition to this, it gives information about the physico-chemical changes that occur in relation to the heat flow and temperature. The magnitude and location of DSC curves inferred the thermal-phase transition of the material. A range of endothermic and exothermic events occur during the decomposition of fibres at different temperatures. It was noted from the DSC curves (Figure 8) that all specimens had a broad curve between the temperature ranges of 46–260°C. These curves accounted for the elimination of water molecules from within the fibre. U1 composites showed thermal stability from 46°C to 146°C and melting temperature (T_m) reached at 500°C. U2 is thermally stable at 48–180°C, and there were no considerable changes observed at above 350°C. In the case of U3, two sharp exothermic peaks were noted at 311°C and 351°C with the area smaller than U1. For the composites T1 (Figure 9), two sharp exothermic peaks at 285°C and 357°C were noted with small area. The melting temperature at 350°C for T2 and 352°C for T3 was noted. No significant changes were observed in T2 and T3 composites above 355°C.

3.7 MA

The existence of microvoids, the type of fibre, the viscous matrix, and the relative humidity were the primary factors that determined the moisture properties. The experimental investigation of MA is used to study the feasibility of composites when it is subjected to false roofing and outdoor applications. Likewise, the qualities of MA could have a direct effect on the mechanical properties of composites. Figure 10 shows the results of MA on the treated/untreated fibre composite specimens versus the percentage of MA after 24 h. As described from Figure 10, the less MA rate was noted for U3 specimens (0.96%), whereas the samples U1 and U2 exhibited the highest MA of 3.22% and 1.44%, respectively. Because the cellulosic components of the fibre are removed from the treated fibre during the alkali treatment process, the treated fibre composites demonstrated a lower MA when compared to U1 to U3. These components are primarily responsible for higher MA (47). As a consequence of the removal of the cellulosic components, a decrease in the proportion of MA may be seen in the treated SFC. The most successful bonding of NaAg with SF was observed in the specimens U3 and T1, with the highest mechanical strength, thus resulting in a decreased MA rate. This could be explained by the fact that there were no gaps between the SF and the NaAg; in other words, compatibility was good for U3 specimen. There was the least degree of variation in the results for the composites (UH1, UH2, UH3, TH1, TH2, TH3). The MA values for each instance are different and were determined arbitrarily. It is interesting to note that 6.46% of MA was noted for alkali-treated, hemp fibre-reinforced epoxy composites (8). Other researcher noted that the moisture content absorption of

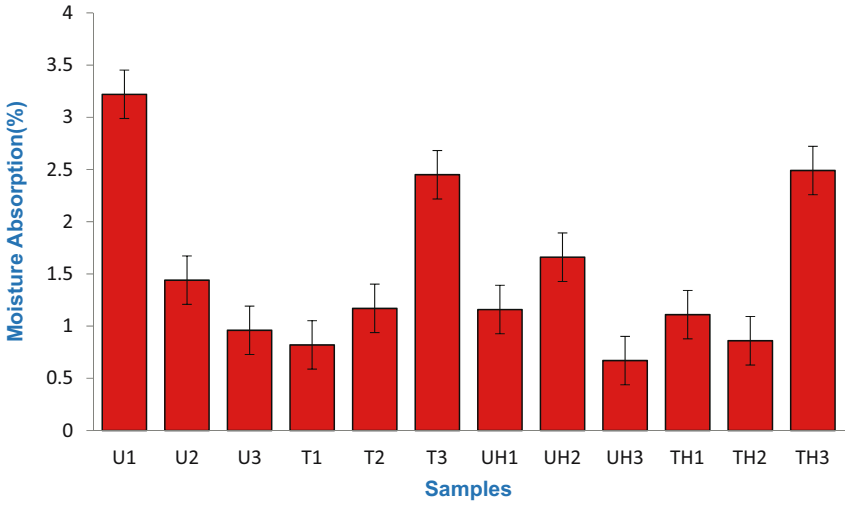

Figure 10: Moisture absorption rate of untreated and treated SF samples.

the sugar palm fibre (SPF)/sugar palm starch biocomposites decreases with increasing fibre loading. It was observed that the composite with 30% of SPF showed an MA of 6% (48). Similarly, in the case of tamarind seed gum, banana fibre composites had 6.5–7.8% MA for various varieties of banana fibre, which suggested that the composite was especially designed for false roofing applications (31).

4 Conclusions

SF-reinforced NaAg gum composites (with different concentrations of gum solution: 1.5%, 2%, and 2.5%) were successfully prepared by the hand lay-up process. The following are the findings that were reached after conducting experiments to study the mechanical, degradation, and morphological aspects of composites. It was inferred that the effect of gum concentration increases the mechanical properties of U3 samples, and it was observed that with heating solution of NaAg provided lower strength when compared to without heating NaAg solution. Biodegradation rate of the treated fibre composites was much faster than that of the untreated fibre composites. Initially, biodegradation was a slow process, but gradually weight loss of untreated/treated SF NaAg composites increased as the number of days of soil incubation period was increased. Biodegradation supports micro-/macrobial activities, thus enriching the soil. Thus, the use of untreated/treated SF-NaAg biocomposites will reduce the environmental issues associated with waste disposal. SEM images of U3 specimen have good interfacial bonding between the fibre and the NaAg gum. The findings of this study lend credence to the role of SF/NaAg biocomposites as potential "ecomaterials." These materials are non-hazardous and have the potential to serve as alternatives to non-biodegradable materials in a variety of non-structural engineering applications, including false roofs, interiors, tablemates, packaging material, low-cost housing, and disposable products. It is recommended that plant fibre composites should be used rather than synthetic fibre composites for the purpose of protecting our environment. At this point, we have developed composites that are superior to conventional materials in every way, including being completely biodegradable, inexpensive, and lightweight. Further research is conducted on the hybridization of the SF composite with the other plant fibres. These fibres, which may include banana and jute fibres, may be tested in an effort to improve the mechanical properties of composites.

Acknowledgements: The authors acknowledge Alagappa Chettiar Government College of Engineering and Technology, Karaikudi, for their help to test the mechanical strength of the composites.

Funding information: The authors state no funding involved.

Author contributions: Balaji Rao Pradeepa prepared manuscript and figures; Amirthalingam V. Kiruthika reviewed the manuscript.

Conflict of interest: The authors state no conflict of interest.

References

(1) Stelescu MD, Manaila E, Craciun G, Chirila C. Development and characterization of polymer eco-composites based on natural rubber reinforced with natural fibers. Materials. 2017;10:787. doi: 10.3390/ma10070787.

(2) Arumugam C, Senthilkumar A, Sarojadevi M. Mechanical, thermal and morphological properties of unsaturated polyester/chemically treated woven kenaf fiber/AgNPs@PVA hybrid nanobiocomposites for automotive applications. J Mater Sci Technol. 2020;9:15298–312. doi: 10.1016/j.jmrt.2020.10.084.

(3) Durowaye SI, Lawal GI, Sekunowo OI, Okonkwo EG. Synthesis and characterisation of hybrid polyethylene terephthalate matrix composites reinforced with Entada mannii fibre particles and almond shell particles. J King Saud Univ Eng Sci. 2018;31:305–13. doi: 10.1016/j.jksues.2017.09.006.

(4) Ashok KG, Kalaichelvan K, Ajith D. Effect of nano fillers on mechanical properties of luffa fiber epoxy composites. J Nat Fibers. 2022;19:1472–89. doi: 10.1080/15440478.2020.1779898.

(5) Sajin JB, Christu PR, Binoj JS, Brailson MB, Gerald ASM, Kheng LG, et al. Impact of fiber length on mechanical, morphological and thermal analysis of chemical treated jute fiber polymer composites for sustainable applications. Curr Res Green Sustain Chem. 2022;5:100241. doi: 10.1016/j.crgsc.2021.100241.

(6) Lokesh P, Surya KTSA, Gopi R, Ganesh BL. A study on mechanical properties of bamboo fiber reinforced polymer composite. Mater Today: Proc. 2020;22:897–903. doi: 10.1016/j.matpr.2019.11.100.

(7) Rapeeporn S, Laongdaw T, Vinod A, Sanjay MR, Suchart S . Agro-waste from Bambusa flexuosa stem fibers: A sustainable and green material for lightweight polymer composites. J Build Eng. 2023;73:106674. doi: 10.1016/j.jobe.2023.106674.

(8) Flavia B, Venanzio G, Enrico A, Raffaele S. Mechanical behavior of chemically-treated hemp fibers reinforced composites subjected to moisture absorption. J Mater Sci Technol. 2023;22:762–75. doi: 10.1016/j.jmrt.2022.11.152.

(9) Delphin P, Anton LR, Darshil US, Christophe B, Alain B. Interfacial and mechanical characterisation of biodegradable polymer-flax fibre composites. Compos Sci Technol. 2021;201:108529. doi: 10.1016/j.compscitech.2020.108529.

(10) Jauhar F, Akmaluddin A, Femiana G. Utilization of kenaf fiber waste as reinforced polymer composites. Results Eng. 2022;13:100380. doi: 10.1016/j.rineng.2022.100380.

(11) Venkatram B, Kailasanathan C, Seenikannan P, Paramasamy S. Study on the evaluation of mechanical and thermal properties of natural sisal fiber/general polymer composites reinforced with nanoclay. Int J Polym Anal Charact. 2016;21:647–56. doi: 10.1080/1023666X.2016.1194616.
(12) Deeban B, Maniraj J, Ramesh M. Experimental investigation of properties and aging behavior of pineapple and sisal leaf hybrid fiber-reinforced polymer composites. e-Polymers. 2023;23:20228104. doi: 10.1515/epoly-2022-8104.
(13) Ramesh M, Rajeshkumar, Lakshmi NR, Nagarajan S, Damodaran VK, Devarajan B. Influence of filler material on properties of fiber-reinforced polymer composites: A review. e-Polymers. 2022;22:898–916. doi: 10.1515/epoly-2022-0080.
(14) Habibur R, Farjana Y, Shadma AK, Zayedul H, Mowshumi R, Muhamad BU, et al. Fabrication and analysis of physico-mechanical characteristics of NaOH treated PALF reinforced LDPE composites: Effect of gamma irradiation. J Mater Res Technol. 2021;11:914–28. doi: 10.1016/j.jmrt.2021.01.067.
(15) Sivasankar GA, Arun KP, Boopathi C, Brindha S, Nirmalraj RJT, Benham A. Evaluation and comparison on mechanical properties of abaca and hemp fiber reinforced hybrid epoxy resin composites. Mater Today Proc. 2023. doi: 10.1016/j.matpr.2023.04.400.
(16) Libo Y, Nawawi C, Liang H, Bohumil K. Effect of alkali treatment on microstructure and mechanical properties of coir fibres, coir fibre reinforced-polymer composites and reinforced-cementitious composites. Const Build Mater. 2016;112:168–82. doi: 10.1016/j.conbuildmat.2016.02.182.
(17) Reshwanth KNGL, Chandrasekar M, Sathish KP, Mohammad J, Reddy DM, Norrrahim MNF, et al. Chapter 8 - Mechanical properties of coir and coir-based hybrid polymeric composites. In: Jawaid M, editor. Woodhead Publishing Series in Composites Science and Engineering, Coir Fiber and its Composites. United Kingdom: Woodhead Publishing; 2022; p. 175–91. doi: 10.1016/B978-0-443-15186-6.00088-6.
(18) Wei C, Qiuying L, Chifei W. The HDPE composites reinforced with waste hybrid PET/cotton fibers modified with the synthesized modifier. e-Polymers. 2022;22:30–7. doi: 10.1515/epoly-2022-0008.
(19) Puttegowda M, Rangappa SM, Jawaid M, Shivanna P, Basavegowda Y, Saba N. Potential of natural/synthetic hybrid composites for aerospace applications. In: M Jawaid, M Thariq, editors. Woodhead Publishing Series in Composites Science and Engineering, Sustainable Composites for Aerospace Applications. United Kingdom: Woodhead Publishing; 2018. p. 315–51. doi: 10.1016/B978-0-08-102131-6.00021-9.
(20) Navin C, Mohammed F. Sisal-reinforced polymer composites. Woodhead Publishing Series in Composites Science and Engineering, Tribology of Natural Fiber Polymer Composites. 2nd edn. In: Navin C, Mohammed F, editors. Woodhead Publishing; 2021. p. 87–110. doi: 10.1016/B978-0-12-818983-2.00003-7.
(21) George M, Abraham TE. Polyionic hydrocolloids for the intestinal delivery of protein drugs: Alginate and chitosan — a review. J Control Release. 2006;114:1–14. doi: 10.1016/j.jconrel.2006.04.017.
(22) Zdiri K, Adel E, Omar H, Mohamed, Jocelyn HB. Properties of recycled PP/clay filaments used for simulation of wastewater treatment filter. J Tex Inst. 2021;112:1753–62. doi: 10.1080/00405000.2020.1841946.
(23) Zdiri K, Cayla A, Elamri A, Erard A, Salaun F. Alginate-based Bio-Composites and their potential applications. J Funct Biomater. 2022;13:117. doi: 10.3390/jfb13030117.
(24) Zdiri K, Elamri A, Harzallah O, Hamdaoui M. Thermo-mechanical characterization of post-consumer PP/Tunisian organo-clay filaments. In: Msahli S, Debbabi F, editors. Advances in Applied Research on Textile and Materials - IX. CIRATM 2020. Springer Proceedings in Materials. Vol 17. Cham: Springer; 2022. doi: 10.1007/978-3-031-08842-1_7.
(25) Zdiri K, Elamri A, Hamdaoui M, Harzallah O, Khenoussi N, Brendlé J. Valorization of post-consumer PP by (Un)modified Tunisian clay nanoparticles incorporation. Waste Biomass Valori. 2020;11:2285–96. doi: 10.1007/s12649-018-0427-2.
(26) Samouh Z, Molnar K, Boussu F, Cherkaoui O, Moznine R. Mechanical and thermal characterization of sisal fiber reinforced polylactic acid composites. Polym Adv Technol. 2019;30:529–37. doi: 10.1002/pat.4488.
(27) Adane AA, Awoke FW. Characterization of Chemically treated sisal fiber/polyester composites. J Eng. 2022;2022:Article ID 8583213, 1–11. doi: 10.1155/2022/8583213.
(28) Agernew M, Mulu BK, Abrha GT. Mechanical and water-absorption properties of sisal fiber (*Agave sisalana*)-reinforced polyester composite. J Nat Fibers. 2019;16:877–85. doi: 10.1080/15440478.2018.1441088.
(29) Parul S, Gupta MK. PLA coated sisal fibre reinforced polyester composite: static and dynamic mechanical properties. Mater Today: Proc. 2018;5:19799–19807. doi: 10.1016/j.matpr.2018.06.343.
(30) Vardhini VKJ, Murugan R, Rathinamoorthy R. Effect of alkali treatment on physical properties of banana fibre. Indian J Fibre Text Res. 2019;44:459–65. https://core.ac.uk/download/pdf/298009346.pdf.
(31) Kiruthika AV, Priyadarzini TRK, Veluraja K. Preparation, properties and application of tamarind seed gum reinforced banana fibre composite materials. Fibers Polym. 2012;13:51–6. doi: 10.1007/s12221-012-0051-x.
(32) Tengsuthiwat J, Boonyasopon P, Dangtungee R, Siengchin S. Characterization of poly(hydroxybutyrate-co-hydroxyvalerate)/Sisal Fiber/Clay bio-composites prepared by casting technique. Period Polytech Mech Eng. 2016;60:103–12. doi: 10.3311/PPme.8721.
(33) Thorsak K, Raminatun M, Emma S, Monica EK, Sigbritt K. Enhancement of mechanical, thermal and antibacterial properties of sisal/polyhydroxybutyrate-co-valerate biodegradable composite. J Met Mater Miner. 2018;28:52–61. doi: 10.14456/jmmm.2018.08.
(34) Sathishkumar TP, Navaneethakrishnan P, Shankar S, Rajasekar R. Investigation of chemically treated randomly oriented sansevieria ehrenbergii fiber reinforced isophthallic polyester composites. J Compos Mater. 2014;48:2961–75. doi: 10.1177/0021998313503589.
(35) Ismail NF, Radzuan NA, Sulong AB, Muhamad N, Haron CH. The effect of alkali treatment on physical, mechanical and thermal properties of kenaf fiber and polymer epoxy composites. Polymers (Basel). 2021;13:2005. https://www.mdpi.com/2073-4360/13/12/2005.
(36) Siddesh NV, Prabakara SS, Raghavendra S. Mechanical properties of sisal fiber reinforced starch based bio composites. AIP Conference Proceedings. Vol. 2057; 2019. p. 020019. doi: 10.1063/1.5085590.
(37) Batista KC, Silva DAK, Coelho LAF, Sergio P, Pezzin APT. Soil biodegradation of PHBV/peach palm particles biocomposites. J Polym Envir on. 2010;18:346–54. doi: 10.1007/s10924-010-0238-4.
(38) Siakeng R, Jawaid M, Asim M, Siengchin S. Accelerated weathering and soil burial effect on biodegradability, colour and texture of

coir/pineapple leaf fibres/pla biocomposites. Polymers. 2020;12:458. doi: 10.3390/polym12020458.
(39) Vasile C, Pamfil D, Râpă M, Darie-Ni,tă RN, Mitelut AC, Popa EE, et al. Study of the soil burial degradation of some PLA/CS Biocomposites. Compos. Part B. 2018;142:251–62. doi: 10.1016/j.compositesb.2018.01.026.
(40) Moriana R, Strömberg E, Ribes A, Karlsson S. Degradation behaviour of natural fibre reinforced starch-based composites under different environmental conditions. J Renew Mater. 2014;2:145–56. doi: 10.7569%2FJRM.2014.634103.
(41) Kumar R, Yakubu MK, Anandjiwala RD. Biodegradation of flax fiber reinforced poly lactic acid. Express Polym Lett. 2010;4:423–30. doi: 10.3144/expresspolymlett.2010.53.
(42) Juntuek P, Chumsamrong P, Ruksakulpiwat Y, Ruksakulpiwat C. Effect of vetiver grass fiber on soil burial degradation of natural rubber and polylactic acid composites. Int Polym Process. 2014;3:379–88. doi: 10.3139/217.2836.
(43) Chin-San W. Preparation, characterization and biodegradability of crosslinked tea plant-fibre-reinforced polyhydroxyalkanoate composites. Polym Degrad Stab. 2013;98:1473–80. doi: 10.1016/j.polymdegradstab.2013.04.013.
(44) Rosa MF, Medeiros ES, Malmonge JA, Gregorski KS, Wood DF, Mattoso LHC, et al. Cellulose nanowhiskers from coconut husk fibers: Effect of preparation conditions on their thermal and morphological behaviour. Carbohydr Polym. 2010;81:83–92. doi: 10.1016/j.carbpol.2010.01.059.
(45) Sina E. Material surface preparation techniques, Surface treatment of materials for adhesion bonding. Vol. 95; 2014.
(46) Kumaran P, Mohanamurugan S, Madhu S, Vijay R, Lenin DS, Sanjay MR, et al. Investigation on thermo-mechanical characteristics of treated/untreated Portunus sanguinolentus shell powder-based jute fabrics reinforced epoxy composites. J Ind Text. 2020;50:427–59. doi: 10.1177/1528083719832851.
(47) Gurdag G, Sarmad S. Cellulose graft copolymers: synthesis, properties, and applications. In: S Kalia, M Sabaa, editors. Polysaccharide based graft copolymers. Berlin, Heidelberg: Springer; 2013. doi: 10.1007/978-3-642-36566-9_2.
(48) Sahari J, Sapuan SM, Zainudin ES, Maleque MA. Mechanical and thermal properties of environmentally friendly composites derived from sugar palm tree. Mater Des. 2013;49:285–9. doi: 10.1016/j.matdes.2013.01.048.